Quantum-classical calculations of X-ray photoelectron spectra of polymers – polymethyl methacrylate revisited

T. Löytynoja,[1,2,a)] I. Harczuk,[2] K. Jänkälä,[1] O. Vahtras,[2] and H. Ågren[2,3]
[1)] *Nano and Molecular Systems Research Unit, University of Oulu, P.O. Box 3000, FIN-90014, Oulu, Finland*
[2)] *Division of Theoretical Chemistry and Biology, School of Biotechnology, Royal Institute of Technology, SE-106 91, Stockholm, Sweden*
[3)] *Laboratory for Nonlinear Optics and Spectroscopy, Siberian Federal University, 660041 Krasnoyarsk, Russia*

In this work we apply quantum mechanics - molecular mechanics (QM/MM) approach to predict core-electron binding energies and chemical shifts of polymers, obtainable via photoelectron spectroscopy (XPS), using polymethyl methacrylate (PMMA) as a demonstration example. The results indicate that standard parametrizations of the quantum part (basis sets, level of correlation) and the molecular mechanics parts (decomposed charges, polarizabilities and capping technique) are sufficient for the QM/MM model to be predictive for XPS of polymers. It is found that the polymer environment produces contributions to the XPS binding energies that are close to monotonous with the number of monomer units, totally amounting to approximately an eV decrease in binding energies. In most of the cases the order of the shifts are maintained, and even the relative size of the differential shifts are largely preserved. The coupling of the internal core-hole relaxation to the polymer environment is found to be weak in each case, amounting only to one or two tenths of an eV. The main polymeric effect is actually well estimated already at the frozen orbital level of theory, which in turn implies a substantial computational simplification. These conclusions are best represented by the cases where the ionized monomer and its immediate surrounding are treated quantum mechanically. If the QM region includes only a single monomer, a couple of anomalies are spotted, which are referred to the QM/MM interface itself and to the neglect of a possible charge transfer.

I. INTRODUCTION

The core-photoelectron chemical shift has been the subject for a great number of theoretical and computational investigations since its discovery in 1963.[1] The ESCA (electron spectroscopy for chemical analysis) model, describing the change of potential at the core due to a charged surrounding, has been instrumental ever since for its interpretation. Over the years several refined models, as well as quantum calculational schemes, have been proposed including those where final state relaxation is accounted for which constitutes the main correction to the original model.[2] In the present work we explore a model where both initial and final state effects and short and long range contributions to the chemical shift are included. We use the QM/MM method where the core-ionization occurs in a central molecule, or group of molecules, described by electronic structure theory, and where the environment is described by atoms equipped with expedient force-fields. This approach transcends previous work on environmental influence on core-electron binding energies (BEs), which have mostly resorted to either supermolecular models, where the environment is successively built up by more quantum mechanical atoms, or by continuum approaches, in particular the self-consistent reaction field method, where the environment is described by a continuum characterized by its dielectric constant.[3] In the QM/MM method the environment is represented by force-field atoms parameterized by decomposed charges (or charge multipoles) and polarizabilities.[4] Such an environment accounts for both initial and final state effects in view of the original ESCA model by a very big cluster of atoms where each atom makes a difference. It thus offers an improvement over the supermolecular model in that many more atoms can be considered, and over the continuum model in that the environmental interaction is granulated and in that initial state charge electrostatic effects are included. The QM/MM model for core-ionization has previously been tested on two aggregates – liquid solutions[5,6] and surface adsorbates[7]. In the present work we make a corresponding study on yet another aggregation, namely polymer fibers.

In order to be useful, a computational model should be flexible to allow for screening of molecules at a relatively low cost, but also generate precision for selected systems. The self-consistent field (SCF) approximation as implemented in Hartree-Fock (HF), multi-configurational self-consistent field (MCSCF) or density functional theory (DFT) is a model that joins efficiency and reasonable accuracy for core-electron BEs, often reaching well within an eV of experimental values. For large molecules each separate chemically unique atom requires its own sequence of SCF cycles to be performed, and from that perspective the well-known Koopmans' theorem, by which all core-electron BEs can be estimated from one ground state optimization by equating them to negative core-orbital energies, is a viable alternative. Such calculations can also be made now in a linear scaling fashion.[8] However, the frozen core BEs obtained by Koopmans'

[a)] Electronic mail: tuomas.loytynoja@oulu.fi

theorem suffer from the well-known relaxation error – the neglect of the energy contribution from the large relaxation of the valence cloud around the created core-hole, generating BE errors ranging up to 30 eV for the first row atoms. For polar or charged systems Koopmans' theorem still often predicts the correct order of the chemical shifts between differently localized core-levels, which might, however, not be the case for unpolar systems, generally showing smaller absolute shifts. It was demonstrated by Bagus that core-states, despite their quasistationary nature, can be optimized separately from the ground state and thus more precise BEs and chemical shifts could be calculated with this, so-called, Δ-SCF method.[9] The main error of the HF Δ-SCF energy refers to correlation error (for non-relativistic systems) which, however, still tends to be quite small since the valence electron cloud remains intact upon core-ionization. An effective way of including (dynamical) correlation is to employ DFT in the Kohn-Sham (KS) approach, which has in fact been very successful when applied to core-ionization BEs[10] and X-ray spectroscopy during recent years. Separate state DFT thus includes dynamical correlation effects for the BEs, in the core-orbital case this refers to correlation of the two core-electrons and the change of correlation energy in the valence cloud due to the relaxation contraction, while near-degenerate type of correlation, as, e.g., found in inner valence ionization, typically does not prevail for core-electron XPS spectra. With the use of SCF calculations Kohn-Sham DFT obviously also requires iterative solutions for each ionization site. One could look for orbital energy predictions, even though Koopmans' theorem is not strictly valid — experience shows that the (negative) orbital energies of the valence shell may mimic experimental BEs quite well.[11] In contrast, for core-orbitals the deviation between orbital energies and true BEs is usually very large, something that can be derived, as first shown by Perdew and Zunger[12], to the neglect of self-interaction for a singly occupied orbital that is much enhanced for orbitals that are strongly localized, like core-orbitals. Different types of corrections to the self-interaction error have been proposed that lead to improved estimation of core BEs with good accuracy using DFT calculations for the ground state of a molecule[13]. Such corrections are, however, beyond the scope of the present paper – here we take interest in chemical shifts and relaxation (internal-QM as well as external-MM) contributions to the shifts. In order to do so without a Koopmans' theorem we define the frozen orbital energy simply as the total energy of the core-state in terms of ground state orbitals. We note that this energy corresponds exactly to the negative of the ground state core-orbital energy in the case of Hartree-Fock (Koopmans' theorem).

Our choice of polymer as demonstration case is PMMA – polymethyl methacrylate, which has been studied widely both experimentally and computationally, for example in Refs.[14–22] This choice is partly dictated by the fact that PMMA is biocompatible and has been used in manufacturing eye lenses employed for cataract disease. Owing to its surface sensitivity, XPS is a useful spectroscopic tool for detecting possible surface aggregation or distortion of the material before it securely can be used. However, in order to make a correct analysis of the spectral outcome it is important to understand how the XPS spectrum of pure PMMA is built up, which structures can be associated to which chemical groups, how to resolve overlapping structures in the spectra etc. Thus it is relevant from a theoretical standpoint to explore the fingerprinting capability of the spectroscopy, but also how precisely the XPS spectrum can be computed. This was the motivation behind a previous work from 1991 where simple model molecules of PMMA were used to explore XPS spectra by means of the Δ-SCF method, and to establish the precision and confidence level for that method.[14,15] Here we extend that study by modeling the full PMMA polymer, where an extended environment to the ionization units are considered and where we now use multiscale QM/MM with DFT for the SCF cycles, and an MM representation by the so-called generalized LoProp approach[23,24] or determining atom or atom-bond charges, multipoles and polarizabilities.

II. CALCULATIONS

To be able to calculate the XPS spectrum of PMMA polymer we first need to find a good estimate for its structure. In principle full sampling of all possible structures should be made, where the BEs are subsequently computed and averaged over the resulting trajectories. This is the so-called integrated approach.[25] In this pilot study we instead choose to examine idealized structures obtained by optimizing a PMMA oligomer consisting of three monomers and to duplicate the geometry of the central unit to build longer chains. We then apply the LoProp approach[23,24] to work out MM force-field parameters. Finally, the core-electron BEs are calculated by using the Δ-SCF method in the QM/MM framework.

A. Structure construction

The starting structure for the three-monomer PMMA oligomer was chosen to be isotactic. It was obtained using the SMILES algorithm implemented in the Avogadro program[26,27] and small adjustments for the positions of the atoms were made to prevent them ending up too close to each other. The structure was further optimized using DFT at the B3LYP[28]/6-31+G*[29–31] level of theory with the Gaussian program[32]. Longer chains were constructed by copying the geometry of the middle monomer while preserving the angles and dihedrals of the carbon backbone chain. Backbone carbons C3 and C5 (see Fig. 2) were capped with hydrogen atoms by placing them in the positions where the next backbone carbons would lie and then scaling the bond lengths to match those of

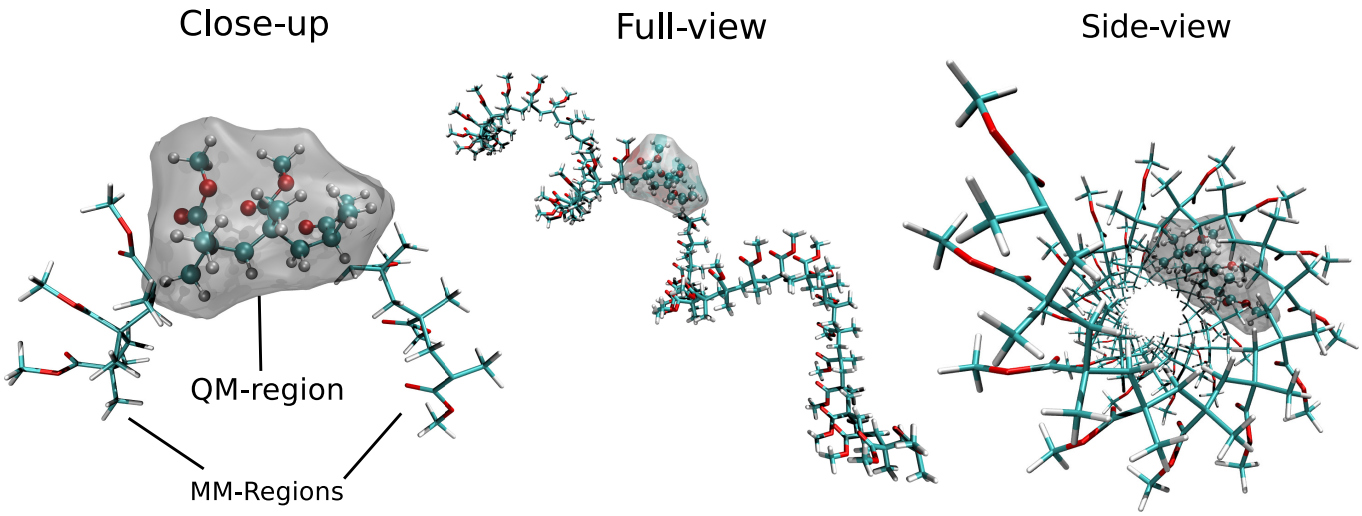

FIG. 1. Core-electron binding energies of PMMA were calculated at various levels of theory, comparing QM and QM/MM structures modeled by modifying the number of monomers in the QM and MM-regions.

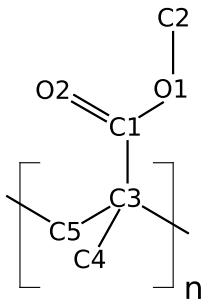

FIG. 2. Labeling of atoms in PMMA monomer. The structure is repeated periodically to produce longer chains.

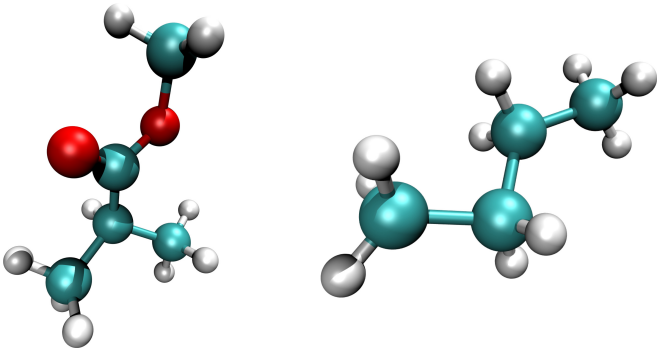

FIG. 3. Capped monomer (left), and conjugate cap fragment (right).

the corresponding hydrogens in the geometry optimized trimer. Hydrogen capping, however, was only applied in MM force-field optimization and not in the QM/MM binding energy calculations to ensure zero net charge of the MM region. The result of the duplicating process is a spiral structure shown in Fig. 1.

B. Optimization of the force-fields

For simplicity the PMMA chain was modeled periodically, which in practice means that properties were obtained for one monomer and then successively repeated along the chain. For the net properties of one final monomer a total of three capped monomers and two conjugate cap fragments were used (see Fig. 3). This is because the backbone carbons C3 and C5 will be present across the three capped monomers. The force-field of the MM region for the QM/MM calculations was computed by employing the MFCC procedure[33], and using the LoProp approach[23,24] to decompose the molecular properties into atomic contributions. Analytical response theory[34] implemented in the Dalton program[8] was applied for the linear polarizability, employing the B3LYP functional with an ANO basis set[35] corresponding to the 6-31+G* contraction. Using MFCC with LoProp, the total property P (charge, dipole-moment, polarizability, etc.) for atom i is obtained from the formula

$$P^i = \sum_j c_j p_j^i, \tag{1}$$

where $c_j = 1$ if the atom appears in a capped monomer, and $c_j = -1$ if the atom is in a conjugate cap joining two monomers. The lower case p_j^i denotes the property of atom i in molecule j. The summation goes over the fragments used in the QM calculation of properties. In this study the obtained MM force-field parameters consist of partial atomic charges and anisotropic polarizabilities. The force-field including charges only is denoted as MM-0 while MM-1 stands for a force-field with both charges and polarizabilities.

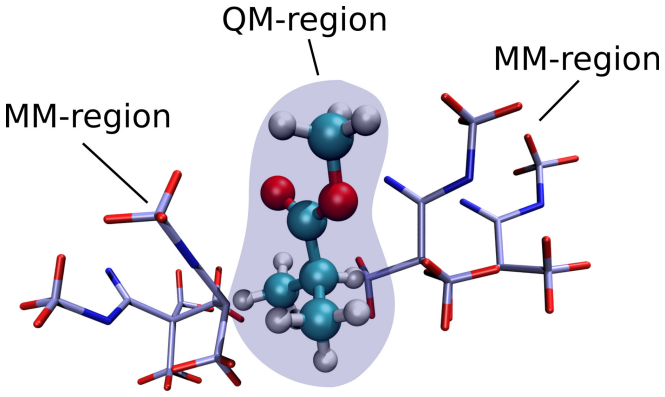

FIG. 4. One monomer in the QM region, calculated with the external potential of 4 monomers in the MM region.

C. QM/MM set up

In PMMA oligomer calculations the QM region consists either of one or three monomers, referred here as 1-QM and 3-QM cases, correspondingly. Fig. 4 showcases a chain of five units with the middle one in the QM region and its two side-monomers in the MM region. In the calculations the length of the PMMA oligomer varied between 1 and 41 monomers. When the chain exceeded the QM region, MM-0 and MM-1 force-fields were applied to the rest of the monomers. One key point to note is that the hydrogen atoms at the ends of the carbon backbone in the QM region do not actually exist in the real polymer structure. These hydrogens were added in the same manner as the capping hydrogen atoms of the whole oligomer (which were not present in the QM/MM calculations as noted earlier) in order to cap the valency of the QM-region, and thus a complicated open-shell electronic structure treatment was avoided. The immediate properties of the carbons located very close to the newly introduced hydrogens were evenly transferred to the closest lying atoms in the MM-region in order to avoid artificial over-polarization. In the MM-1 case the polarizable embedding scheme[36] was used for evaluation of the induced dipole moments. In addition, the interactions between induced dipole moments were damped using Thole's exponential damping scheme[37,38] with the original damping coefficient of 2.1304 to further reduce over-polarization.

D. Core-electron binding energies

Binding energy calculations were performed with the Dalton program[8] by applying the Δ-SCF method[9]. The process started by optimizing the ground state of the system, after which the converged orbitals were used as starting point in a core-hole calculation where the core-orbital was frozen while the other orbitals were allowed to relax. In the last step only the core-orbital was reoptimized. This stepwise technique was applied to prevent the variational collapse of the core-hole wave-function to the lowest valence hole state of that symmetry[39]. Finally, the binding energy was taken to be the difference of total energies of the ground state and the relaxed core-hole state. The procedure was applied for both HF and DFT, referred here as Δ-HF and Δ-DFT, respectively. Both of these quantum methods were also be employed in the QM/MM framework, denoted as Δ-HF/MM and Δ-DFT/MM, accordingly. Additionally, estimates for BEs were obtained using the frozen orbital approximation (Koopmans' theorem for HF wave functions). A frozen orbital energy is defined, in common for HF and DFT, as the core-hole state total energy expressed over the ground state (frozen) orbitals.

In this study *1*s BEs were calculated for two QM oxygen atoms and five QM carbon atoms in the 1-QM case. In the 3-QM case the BEs were computed only for the middle monomer. Dunning's augmented correlation-consistent polarized core-valence triple-ζ (aug-cc-pCVTZ) basis set[40–42] was used in the 1-QM case and in the middle monomer of the 3-QM case. In the latter, the 6-31+G* basis was applied for the other two monomers in order to reduce computation time. Most of the calculations were repeated with both HF and DFT. In DFT the B3LYP exchange-correlation functional was used in all cases. For a review of core-electron binding energies using different functionals we refer to the work of Takahashi and Pettersson[43]. In all cases localized core-hole solutions were employed.

III. RESULTS AND DISCUSSION

Having control over all major intra and extra molecular contributions to the binding energies and chemical shifts, except MM to QM charge transfer, the goal of the present paper is to construct the XPS spectrum of polymer PMMA as closely as possible, and to derive the importance of the different contributions. This also has practical value since there is need to deconvolute the pure PMMA spectrum from contaminated ones, as in the mentioned case where XPS is used to identify clean eye lenses employed for cataract disease. It is also interesting to explore which are the essential parts in order to make polymer calculations of the kind more efficient.

First, it is pertinent to study the performance of the Δ-SCF method for the separate PMMA unit. Indeed this has already been carried for model molecules of PMMA monomer unit for HF and DFT cases in the papers of Brito *et al.*[15] and Triguero *et al.*[10], respectively. These authors could show that the Δ-SCF method gives high accuracy for predicting core-photoelectron chemical shifts for PMMA related model molecules and that core-electron chemical shifts can be obtained within a few tenths of an eV to within an eV of experimental data. This is sufficient accuracy to allow for resolution of spectra in cases when overlapping bands are hard to resolve using experimental information only. As dis-

cussed in those works, the relative success of the Δ-SCF BEs is based on cancellation of errors, which stems from the fact that the valence electron structure is only contracted and not disrupted upon core-electron ionization (see above). Not surprisingly, relaxation was found essential for obtaining the precise shifts while the frozen core or equivalent core (not discussed here) approximations should be taken with "some caution" when aiming at higher precision for the chemical shifts. The role of zero-point vibrational energies (ZPVEs) and relativistic errors were also elucidated. It was also pointed out that for larger molecules the fraction of the ZPVE that should be applied to correct the SCF values grows progressively smaller. It was argued that the absolute value of this correction is relatively constant over the molecules studied and that one can tentatively assume 0.1 eV as a general ZPVE correction that should be subtracted from the computed BEs, with occasionally larger corrections occurring for ionization at sites bonded to hydrogens. It is clear that the functional choice is more pressing than inclusion of the zero-point effect, inflicting variations of many tenths of eVs. The relativistic corrections are comparable or larger than the ZPVEs – estimates from mass-velocity and Darwin relativistic calculations[10] indicate 0.2 eV, 0.3 eV, 0.4 eV and 0.7 eV as corrections for C, N, O and F, respectively – values that are quite atomically inert.

In a polymeric system, as in an unpolar solvent, one can anticipate that the final state effect dominates the environmental contribution to the BE shifts. A first rough estimation is given by the Born model for the solvation energy in a dielectric of a charged sphere with a certain radius. This estimate tends to overshoot the contribution, but depends obviously (and inversely) on the choice of radius. Allowing the medium to react back, in a reaction field model, the shift is modulated compared to the Born model. Granulating the polarization interaction with the solvent is of some importance, e.g. in Ref.[44] ionization shifts in liquid and crystalline benzene was tested versus polarization using central, atom and atom + bond polarizabilities of the external benzene molecules, indicating differences of several tenths of eVs. This distinction is obviously diminished with distance to the ionized molecule. Accounting of the internal core-hole screening is essential for the final polarization estimate. Another salient feature is the differential shift experienced between valence and core-ionization, where the latter is typically stabilized by an additional 0.6–0.8 eV with respect to the valence levels. Thus we realize that there are issues to be addressed by a high level model like QM/MM.

Calculated *1*s core-electron BEs for a single PMMA monomer are presented in Table I. The geometry of the monomer was obtained by capping the middle monomer from the optimized trimer with hydrogen atoms which leads to this structure being slightly unrelaxed. In this paper, the word "single monomer" refers to this unrelaxed structure. The table also includes BEs from the fully optimized PMMA monomer aka the methyl isobutyrate molecule. Comparison between the calculated BEs and experimental methyl isobutyrate values reveals that Δ-DFT performs on average better than Δ-HF, especially in case of the C1 carbon. The deviations are more extensive for oxygen than for carbon atoms, which could partly be understood resulting from the larger relativistic effect. Backbone carbons C3 and C5 are affected most by the relaxation of the monomer geometry, but overall the changes in BEs are small.

One of the most profound issues in QM/MM modeling is the partitioning of the system into QM and MM regions. Like for molecules in solution it is natural for polymers to assign the QM region to one molecular unit – the repeating monomer. Unlike solutions, this unit is chemically bonded to its closest neighbors, which, as shown in the previous section, is handled computationally by a special H-capping technique. Of course in reality the bond can act as a transmitter of charge that helps to screen the created core-hole, a screening that can be assumed to be almost complete. A too small quantum unit may also cause over-polarization of the atoms closest to the QM/MM boundary. In order to put these notions to test we calculated BE shifts with respect to the single monomer BEs for 1-QM/2-MM (one QM monomer, two MM monomers) and 3-QM (no MM region) cases – the results are presented in Table II. For both Δ-HF and Δ-DFT the QM/MM-1 results deviate on average -0.7 eV from the 3-QM values while in the case of QM/MM-0 the deviation is +0.3 eV. In QM/MM-1 the difference is notably large (1.3–1.6 eV) in case of backbone carbons C3 and C5 located near the QM/MM boundary. So indeed the atoms at the edges of the QM region seem to suffer from an interface effect in the QM/MM-1 case.

Figs. 5 and 6 present convergence of the Δ-DFT BEs in the PMMA oligomer as a function of number of monomers in the chain for the 1-QM and 3-QM cases, respectively. In all curves the first point from the left corresponds to a DFT-only calculation while DFT/MM-0 and DFT/MM-1 levels were used for the longer chains. As can be seen, all BEs decrease as the chain is elongated and the largest energy changes occur after inclusion of the first few MM monomers. Closer examination of the curves reveals that even in case of the longest studied chains the BEs are not fully converged, but could presumably decrease by at most 0.0–0.2 eV with an infinitely long polymer. Both MM charges and polarizabilities contribute to the shifts, the latter, however, much more than the former. As noted earlier, in the 1-QM case the inclusion of the MM-1 region causes C3 and C5 BEs to decrease too much, which leads to reverse of order of C3 and C4 BEs. With MM-0 this problem does not occur, but on the other hand the shifts are then very small.

Table III presents the *1*s core-electron BEs obtained with Δ-HF and Δ-DFT methods for a single PMMA monomer and a 41 monomer PMMA oligomer. Long chains were treated at the QM/MM-0 and QM/MM-1 levels of theory. The last two columns depict how much

TABLE I. Calculated and experimental *1*s core-electron binding energies for single PMMA monomer (in eV). In the brackets are errors to the experimental values of gas phase methyl isobutyrate.

Method	O1	O2	C1	C2	C3	C4	C5
Δ-HF[a]	538.46 (−0.87)	536.80 (−1.00)	295.24 (0.81)	292.63 (0.25)	291.27 (0.2)	290.73 (0.0)	290.51 (−0.2)
Δ-HF[b]	538.52 (−0.81)	536.74 (−1.06)	295.21 (0.78)	292.64 (0.26)	291.10 (0.0)	290.82 (0.1)	290.66 (0.0)
Δ-DFT[a]	538.74 (−0.59)	537.12 (−0.68)	294.41 (−0.02)	292.48 (0.10)	291.22 (0.1)	290.70 (0.0)	290.51 (−0.2)
Δ-DFT[b]	538.78 (−0.55)	537.06 (−0.74)	294.38 (−0.05)	292.49 (0.11)	291.08 (0.0)	290.78 (0.1)	290.65 (−0.1)
Expt.[c]	539.33	537.80	294.43	292.38	291.1	290.7	290.7

[a] The structure is that of the middle monomer from the geometry optimized trimer with additional capping hydrogens. It can be assumed to have nearly relaxed methyl isobutyrate geometry.
[b] Fully relaxed methyl isobutyrate geometry
[c] Gas phase methyl isobutyrate from Ref.[15]

TABLE II. PMMA three monomer oligomer *1*s binding energy shifts with respect to single monomer QM-only cases (in eV).

System	Method	O1	O2	C1	C2	C3	C4	C5
1-QM/2-MM	Δ-HF/MM-0	−0.23	−0.37	−0.28	−0.17	−0.05	−0.03	−0.05
1-QM/2-MM	Δ-HF/MM-1	−0.81	−1.07	−1.04	−0.56	−1.76	−0.92	−1.84
3-QM	Δ-HF	−0.31	−0.56	−0.45	−0.25	−0.38	−0.55	−0.28
1-QM/2-MM	Δ-DFT/MM-0	−0.22	−0.34	−0.26	−0.17	−0.06	−0.03	−0.05
1-QM/2-MM	Δ-DFT/MM-1	−0.83	−1.05	−1.03	−0.57	−1.70	−0.90	−1.79
3-QM	Δ-DFT	−0.37	−0.59	−0.50	−0.28	−0.42	−0.60	−0.37

the atom–atom BE shifts deviate on average from the experimental solid PMMA shifts, which in essence describes how well the calculations capture the shape of the experimental spectrum. Of course, any errors produced by the fitting process in the experiments introduce errors to these numbers as well. Remarkably, in our calculations, a good shape of the spectrum seems to be given already by a single monomer Δ-DFT calculation, indicating that qualitatively good results can indeed be obtained with rather small effort. Larger errors in the Δ-HF spectrum are mostly caused by the C1 BE. The introduction of the MM region shifts the BEs to lower magnitudes as is expected from polymerization. The shapes of the spectra are worst for the 1-QM case on QM/MM-1 level in which especially the backbone carbon BEs decrease too much. This can be further confirmed from Table IV, which shows the BE shifts for each orbital with respect to the single monomer cases. The average shift of the BEs induced by polymerization in Δ-DFT/MM-1 calculations is -1.58 eV, which can be decomposed to -0.42 eV and -1.16 eV shifts from MM charges and polarization, correspondingly. However, the latter value is probably somewhat too large due to the QM/MM interface effect, as discussed earlier. More realistic values could be obtained from the C2 atom as it is furthest away from the interface. It has total shift of -1.03 eV with charge and polarization contributions of -0.42 eV and -0.61 eV.

In the 3-QM case, however, the spectral shapes are very similar between pure QM and QM/MM-1 level calculations. Once again, DFT performs better than HF. Notably, the C2 BE, being furthest away from the carbon backbone, is perturbed the least by the MM region. In the paper by Brito *et al.* the polymer shifts are estimated using a group shift method, which results in values -0.3 eV, -0.07 eV, -0.6 eV, -0.3 eV and -0.6 eV for C1–C5, respectively.[15] In comparison, our Δ-QM/MM-1 shifts are all larger in magnitude by about 0.5 eV – 0.9 eV and C1 and C4 do not shift less than C3 and C5. However, there is agreement in that the C2 BE is shifted by the least amount. Interestingly, if values from relaxed monomer geometry are used instead, C3 BE is estimated to shift as little as C2 BE. If polymer BEs calculated with DFT are compared to solid PMMA experimental values, it is seen that C2 has the largest shift, which would suggest it having the vastest changes in its environment when the structure if solidified. The average shift generated by polymerization is -1.04 eV for Δ-DFT. This can be broken down to -0.45 eV, -0.24 eV and -0.35 eV contributions from additional QM monomers, MM charges and polarizabilities, respectively. Brito *et al.* obtained the experimental BEs by fitting five separate peaks to the carbon *1*s region. We note here that if their four peak fit values (C4 and C5 with equal BEs) would be used instead as reference to calculate the numbers in the last column of Table III, the 3-QM shift errors would decrease by roughly 0.1 eV.

Table V shows the relaxation energies between BEs obtained using the frozen core approximation and after relaxation of the orbitals in the 1-QM case. As can be seen, the changes are large and thus frozen core BEs do not produce good absolute BEs. The values are ~22 eV off from the relaxed ones in the oxygen case and 14–

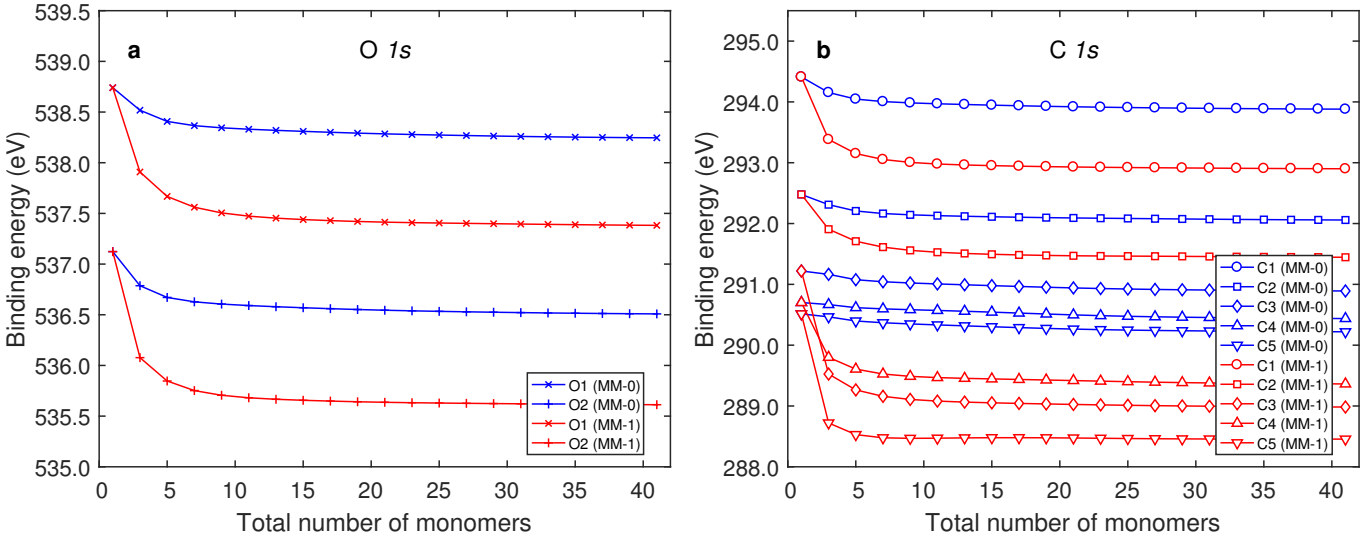

FIG. 5. Convergence of binding energies as a function of PMMA oligomer length in calculations with one DFT monomer. The MM part was modeled using partial atomic charges (MM-0 level) and charges and anisotropic polarizabilities (MM-1 level).

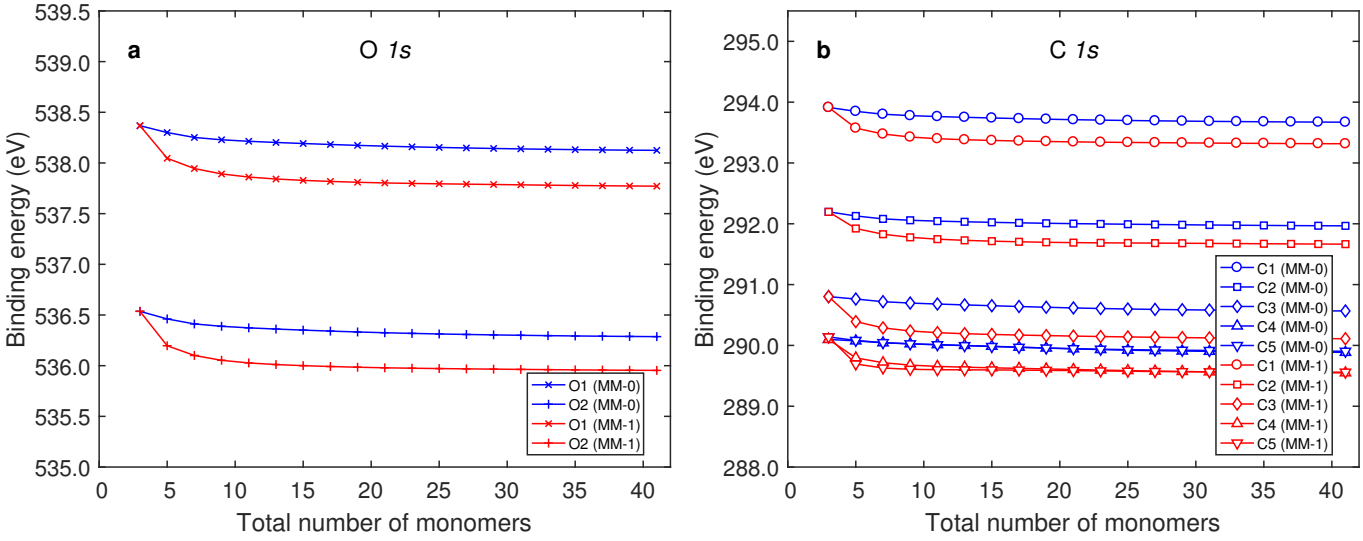

FIG. 6. Convergence of binding energies as a function of PMMA oligomer length in calculations with three DFT monomers. The MM part was modeled using partial atomic charges (MM-0 level) and charges and anisotropic polarizabilities (MM-1 level).

15 eV the in the carbon case. Differences between single monomer and QM/MM-0 results are minuscule, but after addition of the polarizabilities the relaxation energies get slightly smaller. There is somewhat more relaxation in case of DFT than HF BEs.

Figs. 7 and 8 present convergence of the frozen core BEs as a function of PMMA chain length for the 1-QM and 3-QM cases, respectively. It is clear that the frozen orbital energies make up for the major polymer effect on the XPS spectra, amounting to an order of magnitude larger effect than the corresponding relaxation dependence (see below). Both MM charges and polarizabilities contribute to the frozen orbital shifts, however, the latter ones have much larger impact. The convergence with respect to MM units is in almost all cases close to monotonous and the original shift order is maintained with one exception. The exception refers to the 1-QM case where there actually is a swap of shift order between C3 and C4. However, going to the 3-QM case, the order of those two entries are maintained, and with almost identical difference. This is a valuable piece of information as it indicates that a prediction of the environmental contribution to a pure polymer spectrum can be obtained already in the frozen orbital picture. This would be a significant simplification in terms of efficiency in calculations of polymer XPS spectra, although still

TABLE III. PMMA monomer and oligomer *1*s binding energies (in eV)

System	Method	O1	O2	C1	C2	C3	C4	C5	$O_{Err.}$ [a]	$C_{\langle Err.\rangle}$ [b]
1-QM	Δ-HF	538.46	536.80	295.24	292.63	291.27	290.73	290.51	0.16	0.39
1-QM/40-MM	Δ-HF/MM-0	537.97	536.15	294.68	292.20	290.94	290.47	290.21	0.31	0.24
1-QM/40-MM	Δ-HF/MM-1	537.12	535.27	293.73	291.60	288.97	289.37	288.41	0.35	0.84
3-QM	Δ-HF	538.15	536.24	294.79	292.38	290.88	290.18	290.23	0.41	0.43
3-QM/38-MM	Δ-HF/MM-0	537.91	535.99	294.55	292.15	290.65	289.97	289.99	0.42	0.42
3-QM/38-MM	Δ-HF/MM-1	537.56	535.68	294.22	291.85	290.18	289.63	289.64	0.39	0.45
1-QM	Δ-DFT	538.74	537.12	294.41	292.48	291.22	290.70	290.51	0.12	0.15
1-QM/40-MM	Δ-DFT/MM-0	538.25	536.51	293.88	292.06	290.89	290.44	290.22	0.24	0.19
1-QM/40-MM	Δ-DFT/MM-1	537.38	535.61	292.90	291.45	288.98	289.36	288.46	0.27	0.63
3-QM	Δ-DFT	538.37	536.54	293.91	292.20	290.80	290.10	290.14	0.33	0.30
3-QM/38-MM	Δ-DFT/MM-0	538.12	536.29	293.67	291.97	290.57	289.89	289.90	0.34	0.29
3-QM/38-MM	Δ-DFT/MM-1	537.77	535.95	293.32	291.67	290.11	289.55	289.56	0.32	0.30
Methyl isobutyrate	Expt.[c]	539.33	537.80	294.43	292.38	291.1	290.7	290.7		
Solid PMMA	Expt.[c]	530.2	528.7	285.9	283.7	282.5	282.2	281.9		

[a] Absolute deviation of the calculated O1–O2 shift from the corresponding experimental solid PMMA shift.
[b] Mean absolute deviation of the calculated C–C shifts from the corresponding experimental solid PMMA shifts. Includes all ten pairs.
[c] From Ref.[15]

TABLE IV. PMMA oligomer *1*s binding energy shifts with respect to single monomer QM-only cases (in eV)

System	Method	O1	O2	C1	C2	C3	C4	C5
1-QM/40-MM	Δ-HF/MM-0	−0.50	−0.65	−0.56	−0.42	−0.33	−0.26	−0.30
1-QM/40-MM	Δ-HF/MM-1	−1.34	−1.53	−1.51	−1.02	−2.30	−1.36	−2.10
3-QM	Δ-HF	−0.31	−0.56	−0.45	−0.25	−0.38	−0.55	−0.28
3-QM/38-MM	Δ-HF/MM-0	−0.55	−0.81	−0.69	−0.48	−0.62	−0.76	−0.52
3-QM/38-MM	Δ-HF/MM-1	−0.90	−1.12	−1.02	−0.77	−1.09	−1.10	−0.86
1-QM/40-MM	Δ-DFT/MM-0	−0.49	−0.61	−0.53	−0.42	−0.33	−0.26	−0.29
1-QM/40-MM	Δ-DFT/MM-1	−1.36	−1.51	−1.51	−1.03	−2.24	−1.34	−2.06
3-QM	Δ-DFT	−0.37	−0.59	−0.50	−0.28	−0.42	−0.60	−0.37
3-QM/38-MM	Δ-DFT/MM-0	−0.62	−0.84	−0.74	−0.51	−0.65	−0.82	−0.61
3-QM/38-MM	Δ-DFT/MM-1	−0.97	−1.17	−1.09	−0.81	−1.11	−1.15	−0.95

separate core-hole state calculations must be made for the free monomer to catch the internal relaxation, which is crucial for the shifts.

Our model also allows to scrutinize how the relaxation energy is coupled to a polymeric environment. The convergence of the relaxation energies as function of PMMA oligomer length are plotted in Figs. 9 and 10 where the DFT regions involve one and three monomers, respectively. One first notes that this coupling is very small at the MM-1 level (MM charges and polarizabilities), one or two tenths of eVs at most, compared with the total relaxation, while with MM-0 (MM charges only) the coupling is close to zero. The relaxation behavior with respect to polymer length is monotonous, and with only one exception the order of the relaxation energies is maintained throughout the series. However, there is one salient feature in this comparison, namely that the relaxation energy reduces in magnitude from 1 to 3 monomers in the 1-QM quantum case, while after 3 monomers, in both 1-QM and 3-QM cases, the relaxation is increased almost monotonously. One could here speculate that the relaxation becomes incomplete due to artificial electrostatic interaction with the closest MM units, or that the charge penetration to the core is altered by these units. It would require a special study to sort this out.

An analysis of negative Kohn-Sham orbital energies was also made. As mentioned in the introduction there is no counterpart to Koopmans' theorem in the case of core-electron BEs because of the large self-correction errors. The variations of core-orbital energies with respect to chemical surrounding have still been empirically used to predict XPS shifts[45,46]. In contrast to frozen core BEs these (negative of core-orbital eigenvalues – COEs) values are lower than Δ-DFT BEs by 12–18 eV. To check how well the different methods produce shifts and shapes of the experimental spectra, mean absolute errors for atom-atom shifts were calculated for a couple of systems in the same manner as in the last two columns of Table III. In case of the O *1*s level in gas phase methyl isobutyrate molecule this produces deviations of 0.14 eV,

TABLE V. Relaxation energies between frozen core and relaxed Δ-SCF *1s* core-hole states in 1-QM monomer cases (in eV)

System	Method	O1	O2	C1	C2	C3	C4	C5
1-QM	Δ-HF	−22.08	−22.18	−14.33	−14.45	−15.10	−14.71	−14.75
1-QM/40-MM	Δ-HF/MM-0	−22.07	−22.18	−14.34	−14.46	−15.10	−14.71	−14.75
1-QM/40-MM	Δ-HF/MM-1	−21.88	−22.09	−14.10	−14.48	−14.85	−14.61	−14.52
1-QM	Δ-DFT	−22.27	−22.31	−14.74	−14.67	−15.26	−14.88	−14.90
1-QM/40-MM	Δ-DFT/MM-0	−22.26	−22.31	−14.73	−14.68	−15.27	−14.88	−14.91
1-QM/40-MM	Δ-DFT/MM-1	−22.08	−22.24	−14.51	−14.70	−14.98	−14.76	−14.65

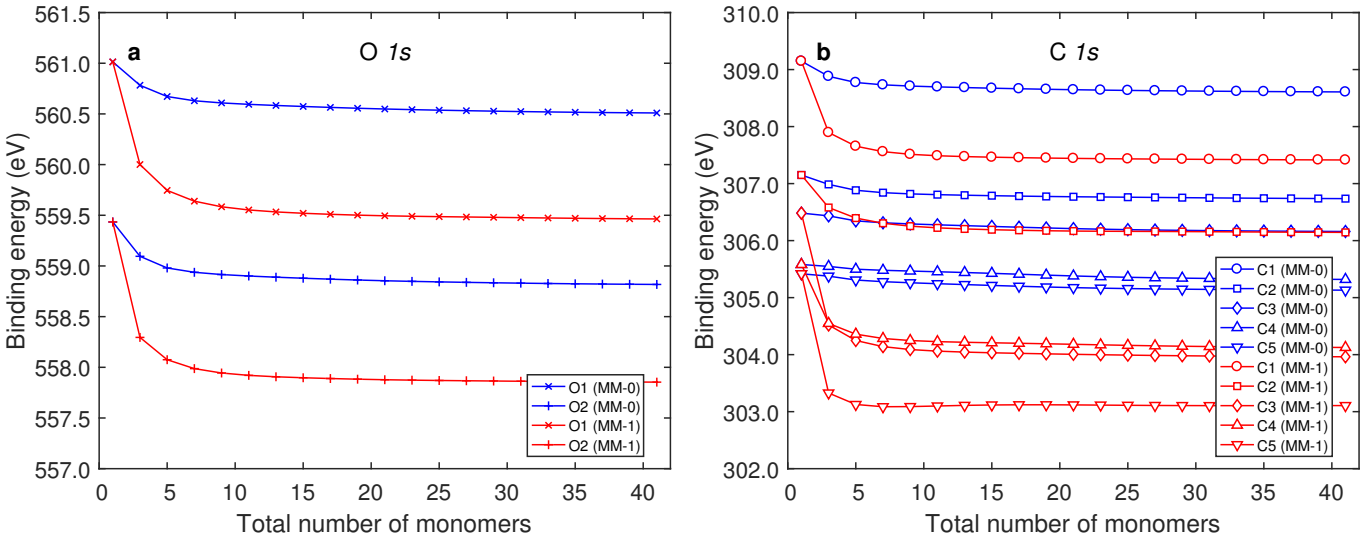

FIG. 7. Convergence of the frozen core binding energies as a function of PMMA oligomer length in calculations with one DFT monomer. The MM part was modeled using partial atomic charges (MM-0 level) and charges and anisotropic polarizabilities (MM-1 level).

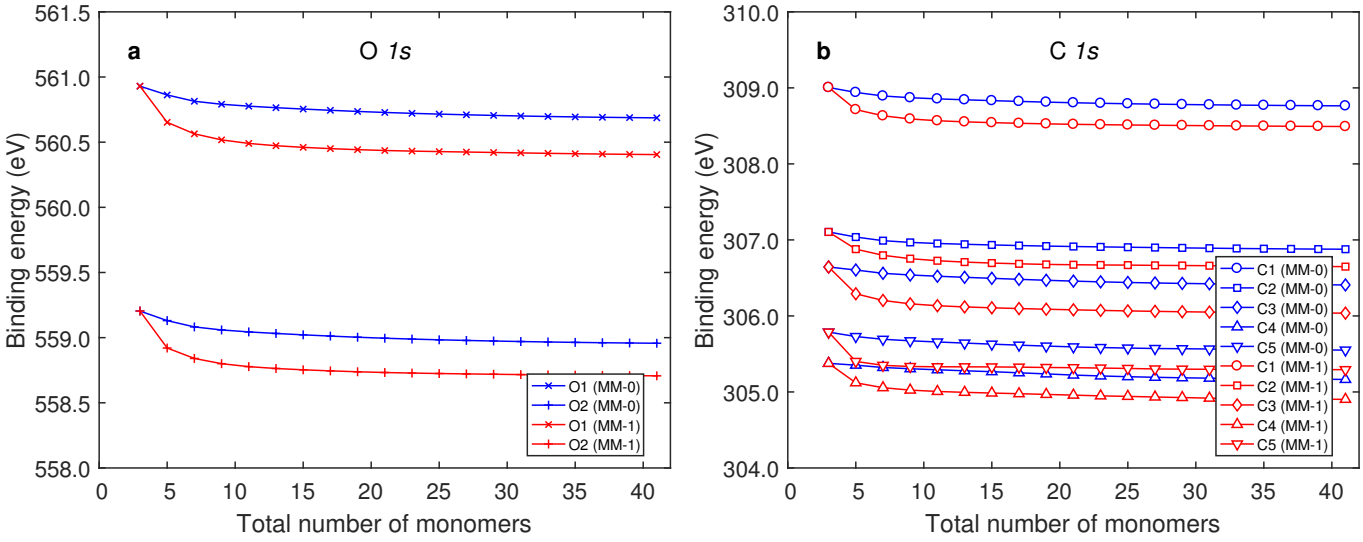

FIG. 8. Convergence of the frozen core binding energies as a function of PMMA oligomer length in calculations with three DFT monomers. The MM part was modeled using partial atomic charges (MM-0 level) and charges and anisotropic polarizabilities (MM-1 level).

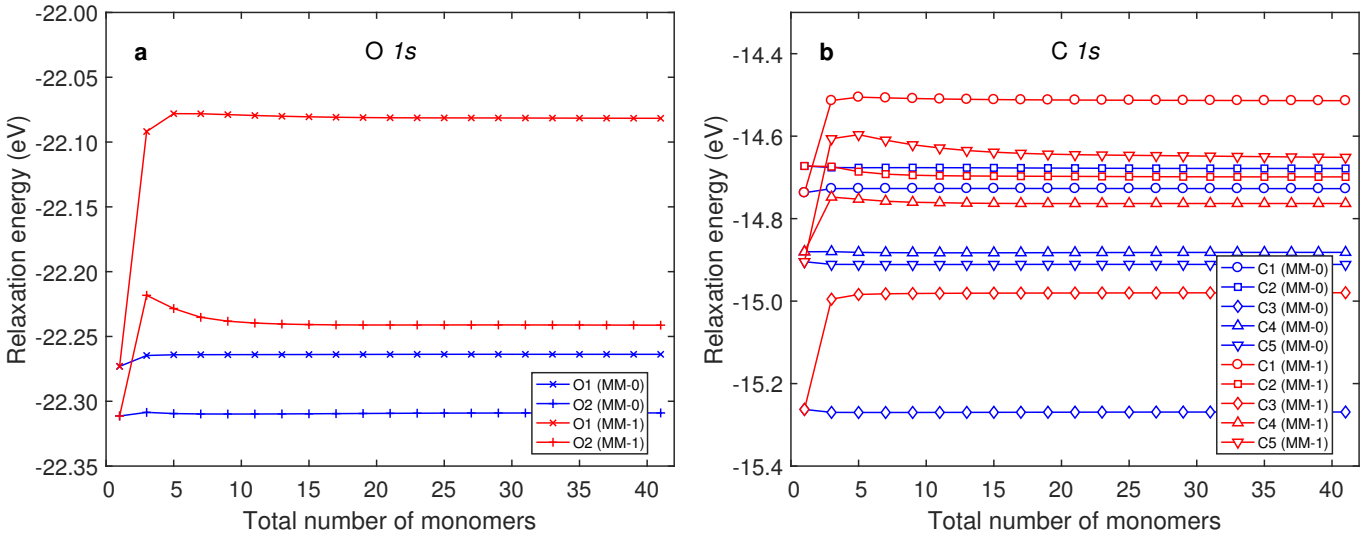

FIG. 9. Convergence of the relaxation energies as a function of PMMA oligomer length in calculations with one DFT monomer. The MM part was modeled using partial atomic charges (MM-0 level) and charges and anisotropic polarizabilities (MM-1 level).

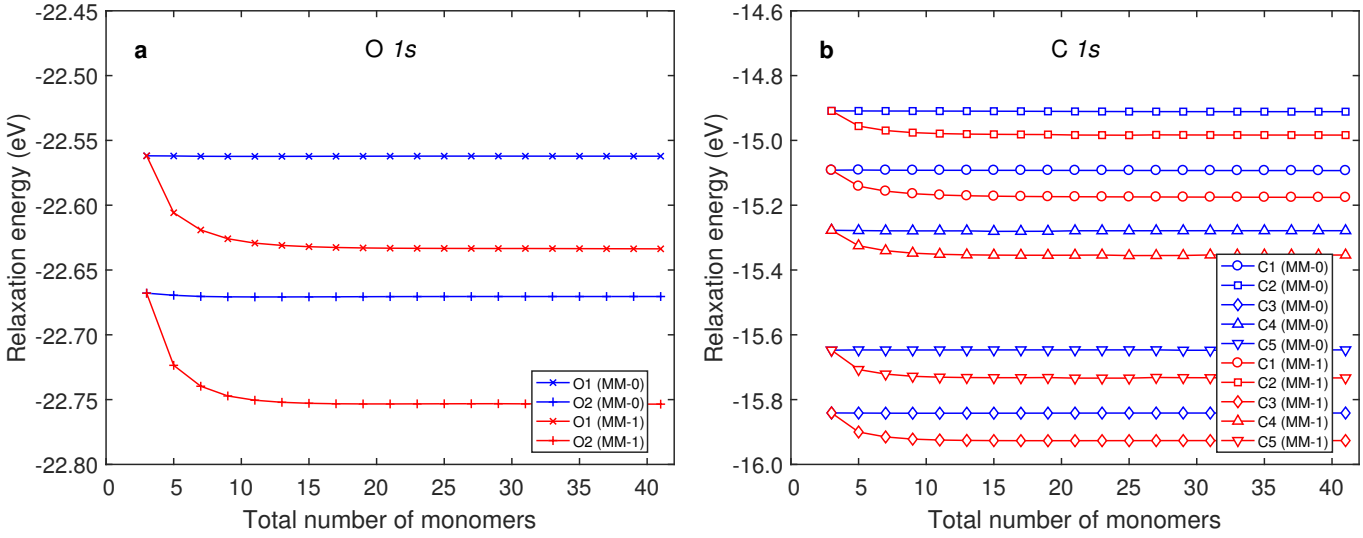

FIG. 10. Convergence of the relaxation energies as a function of PMMA oligomer length in calculations with three DFT monomers. The MM part was modeled using partial atomic charges (MM-0 level) and charges and anisotropic polarizabilities (MM-1 level).

0.13 eV and 0.19 eV from the experiments when using BEs obtained from COE, frozen core approximation and Δ-DFT method, respectively. For C *1*s the corresponding numbers are 0.24 eV, 0.24 eV and 0.09 eV. For the sake of completeness we report errors of 0.14 eV and 0.25 eV for O *1*s and 0.24 eV and 0.38 eV for C *1*s from HF Koopmans' theorem and Δ-HF method, accordingly. Therefore, on average it seems that Δ-DFT gives slightly better match to the shape of the experimental spectrum than the other applied methods. In addition, frozen core and COE produce very similar deviations in DFT framework and, as a matter of fact, the BEs between the two methods differ with a close approximation by a constant when the O *1*s and C *1*s regions are considered separately (39.32 eV and 28.87 eV shifts), with deviations less than 0.01 eV. At the MM-1 level in the longest polymer case (3 QM monomers, 38 MM monomers) this number increases to over 0.1 eV. The deviations related to the spectral shape are 0.19 eV, 0.20 eV and 0.32 eV for O *1*s and 0.57 eV, 0.52 eV and 0.30 eV for C *1*s with the different methods. At the MM-0 level the results resemble those in the case of gas phase methyl isobutyrate. The COEs require only a ground state calculation and are thus very easy to execute and do not require much computational effort in comparison to the other methods. It was demonstrated by Giebers *et al.* that this kind of Koopmans' theorem based approach combined with a natural bond orbital analysis and a linear fitting process provides an accurate and easy to use tool to calculate C *1*s BEs of organic monolayers[45]. With this method they were able to obtain 0.29 eV average absolute error for the BEs. Further improvements to Koopmans' theorem based BEs can also be made. For example, Leftwich and Teplyakov corrected N *1*s BEs with values that linearly depend on the partial charge of the nitrogen atom reaching as low as 0.17 eV average absolute error[46]. After these models have been fitted against known experimental values they can be used for BE predictions of new molecules as well. The fitting parameters will of course have to be revaluated for different environments. To make fully first principle predictions the environment needs to be accounted explicitly by some means, for instance with QM/MM. Furthermore, if absolute core-level BEs are of interest, the missing relaxation of the ionic state has to be addressed, which is the strength of Δ-SCF method over Koopmans' theorem.

Finally, the calculated Δ-DFT BEs for a single monomer and PMMA chain (3-QM/38-MM, MM-1 case) were transformed into spectra by modeling the peaks with Gaussian functions. To help the comparison, the polymer spectra were uniformly shifted by -0.97 eV and -1.09 eV to match O1 and C1 peaks of the monomer, accordingly. All the peaks were chosen to have the same intensity and 1.1 eV width which corresponds to the FWHM value of the C1 peak in experimental solid PMMA XPS spectrum by Brito *et al.*[15]. In reality the peaks evidently have non-equal areas and asymmetric characteristics. The calculated spectra are shown in Fig. 11. For oxygen atoms the polymerization widens the BE gap in the calculated spectrum. This effect can also be seen when comparing experimental BEs from methyl isobutyrate and solid PMMA, even though the shift is smaller.[15] In case of calculated carbon BEs, C2 is affected least by the polymerization causing it to move in relation to the other carbon peaks. In comparison to the solid PMMA experiments, this actually makes the shape of the spectrum look slightly worse than in the one monomer calculation. In the gas phase methyl isobutyrate experiment no shift is observed between C4 and C5 BEs, while our monomer calculation shows a 0.19 eV difference. In a fully relaxed geometry the shift shrinks down to 0.13 eV. In the work of Brito *et al.* proper fitting strategies of the carbon peaks in solid PMMA spectrum are discussed. They suggest a five separate peak fit to be the most appropriate for the C *1*s region, but we note here that setting C4 and C5 peaks equal could also give a reasonable result. Our calculations show that the shifts between monomer and polymer are remarkably close for different ionization sites and thus that a common shift to align the spectra works well. This is an important conclusion of the present work, and indicates that a higher level calculation of a trimer unit can be used as basis to assign the pure polymer spectrum.

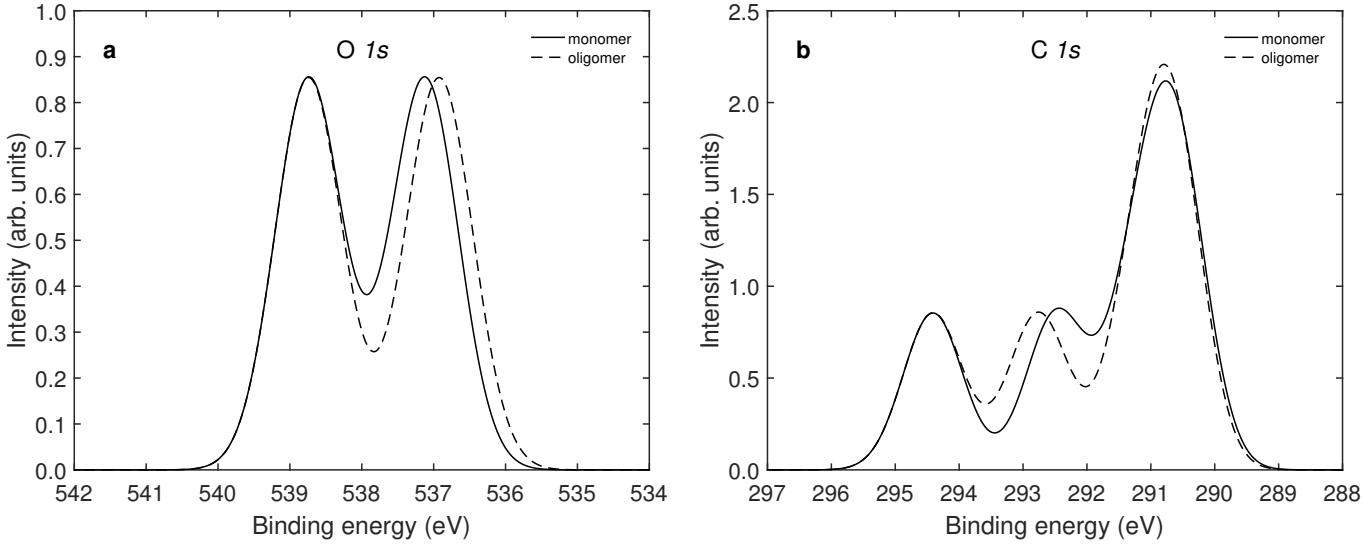

FIG. 11. Calculated O *1*s and C *1*s spectra for single PMMA monomer (solid line) and for chain with 41 monomers (dashed line). The spectra were formed by convoluting the peaks obtained from Δ-DFT calculations with Gaussian functions with 1.1 eV width. Oligomer spectra were shifted along the x-axis to match O1 and C1 binding energies of the monomer spectra. For more information, see the text.

IV. CONCLUSIONS

The present work was motivated by the possibilities offered by modern quantum-classical, multiscale, modelling of molecules and materials, including a wide range of properties. We took interest in the use of the quantum mechanics molecular mechanics method (QM/MM) in X-ray photoelectron spectra (XPS) where the core-ionization occurs in a specific atom, which together with its nearest surrounding is described by electronic structure theory and where the outer environment is described by atoms equipped with classical force-fields, generally parameterized in terms of local charges and polarizabilities. This approach is the most general to date to study environmental effects on XPS spectra as it includes short as well as long range effects, and, in view of the original ESCA models, both initial and final state effects. The QM/MM model for core-ionization has previously been tested on two aggregates – liquid solutions and surface adsorbates – in the present work we applied the technology to a third aggregate – polymer fibers. We chose polymethyl methacrylate (PMMA) as demonstration example, as the XPS spectra of this species has been used in practical applications, where it is desirable to predict a pure spectrum, and because its monomer unit has been the subject for previous work, upon which we here can build to explore the polymer environment effect. The technical work behind the present study rests on previous experience in quantum chemistry calculations of XPS as well as of recent advances in parameterizations of the molecular mechanics forces-fields.

Several conclusions of both general and detailed character can be drawn from this pilot study. One goal of this work was to study how well the shape of the solid PMMA spectrum can be reproduced using a simple polymer as an approximation for the structure. While even a single monomer, pure QM calculations can do this very well, the long range interactions are still required for the full polymer shifts, which, as predicted by our QM/MM calculations, are approximately -1 eV for carbon and oxygen *1*s orbitals with respect to the single monomer calculation. The C2 atom, the one furthest away from the carbon backbone, has a notably smaller shift than the rest of the atoms, while BEs of the C4 and C5 atoms end up being almost equal. Essentially the polymer environment produces a monotonous decrease of the BEs with respect to the number of monomer units, making it easy to extrapolate a small remaining part to infinity. Alternatively, one could apply a dielectric continuum for the very long range contributions. In most cases of the tested PMMA polymer structure the order of the shifts are maintained and even the relative size of the differential shifts are kept intact. Although the generality of this statement must be put to further test for different kinds of polymers, it nevertheless indicates that good first estimates of the polymer spectrum can be obtained by few, or even by one, monomer units. The main polymeric effect actually emerges at the frozen orbital level of theory, as the coupling of the internal core-hole relaxation to the polymer environment is found to be weak, amounting only to one or two tenths of an eV. This in turn implies a substantial computational simplification. We have also tested a simplifying procedure of using the negative core-orbital energies from DFT ground state calculations (corresponding to Koopmans' theorem in case of Hartree-Fock) which have previously been applied, for example,

by Giesbers *et al.*[45] and by Leftwich and Teplyakov[46]. We find that this procedure gives results quite similar to the frozen orbital approximation concerning the shifts and the shapes of the spectra.

We have tested two quantum descriptions where either one or three monomers are included in the quantum mechanical treatment. In calculations with one QM monomer a couple of anomalies are spotted, which are referred to the QM/MM interface itself, and neglect of a possible charge transfer. Despite the applied damping, cutting chemical bonds with the QM/MM boundary may lead to over-polarization introduced by core-hole atoms close to the boundary, causing their BEs to decrease too much. However, we found these problems to be substantially reduced when the QM region was extended to cover three monomers, so adding a QM buffer between the boundary and core-hole atoms. Thus, the three QM monomer results should be considered to be the most accurate ones. The -1 eV polymerization shift in the three QM monomer case cannot be strictly divided into parts from MM charges and polarizabilities, because the shift includes contributions from the additional QM monomers as well. In the one monomer case, on the other hand, the usage of polarizabilities results in too low average polymerization shift, but using the BE of the C2 atom, the contributions can be estimated to be about -0.4 eV and -0.6 eV from MM charges and polarizabilities, accordingly.

Our conclusions should also be qualified by that we made the common assumption that at high X-ray photon energies, transcending the ionization edge by 50 eV or more; there is no "chemical shift" of the core-electron ionization cross section. We stress that here we have studied the 1-dimensional chain dependence of the XPS spectra. For absolute BEs in solid state polymer spectra 3-dimensional calculations should be carried out, which is trivial, but also a qualified estimate of the so-called work function for the photoelectron should be made, which is non-trivial. The work function is though expected to apply uniformly to all elements of the same type and to not to perturb the core shifts. By large, this pilot study is supportive of the applicability of the quantum classical QM/MM for predicting X-ray photoelectron spectra of general polymeric systems.

ACKNOWLEDGMENTS

This work was financially supported by Vilho, Yrjö and Kalle Väisälä foundation and University of Oulu Graduate School. Computational resources were provided by CSC – IT Center for Science administrated by the Ministry of Education and Culture of Finland and the Swedish National Infrastructure for Computing (SNIC) for the project "Multiphysics Modeling of Molecular Materials" (SNIC 2014/11-31 and SNIC 2015/16-10). We acknowledge The Knut and Alice Wallenberg foundation for financial support (Grant No. KAW-2013.0020). We thank Professor Yaoquan Tu for his insight about the structure of the PMMA polymers.

[1] K. Siegbahn, C. Nordling, G. Johansson, J. Hedman, P. F. Hedén, K. Hamrin, U. Gelius, T. Bergmark, L. O. Werme, R. Manne, and Y.Baer, *ESCA applied to free molecules* (North-Holland Pub. Co., 1969).
[2] H. Ågren, Int. J. Quantum Chem. **39**, 455 (1991).
[3] H. Ågren, C. M. Llanos, and K. V. Mikkelsen, Chem. Phys. **115**, 43 (1987).
[4] C. B. Nielsen, O. Christiansen, K. V. Mikkelsen, and J. Kongsted, J. Chem. Phys. **126**, 154112 (2007).
[5] J. Niskanen, N. Arul Murugan, Z. Rinkevicius, O. Vahtras, C. Li, S. Monti, V. Carravetta, and H. Ågren, Phys. Chem. Chem. Phys. **15**, 244 (2013).
[6] T. Löytynoja, J. Niskanen, K. Jänkälä, O. Vahtras, Z. Rinkevicius, and H. Ågren, J. Phys. Chem. B **118**, 13217 (2014).
[7] T. Löytynoja, X. Li, K. Jänkälä, Z. Rinkevicius, and H. Ågren, J. Chem. Phys. **145**, 024703 (2016).
[8] K. Aidas, C. Angeli, K. L. Bak, V. Bakken, R. Bast, L. Boman, O. Christiansen, R. Cimiraglia, S. Coriani, P. Dahle, E. K. Dalskov, U. Ekström, T. Enevoldsen, J. J. Eriksen, P. Ettenhuber, B. Fernández, L. Ferrighi, H. Fliegl, L. Frediani, K. Hald, A. Halkier, C. Hättig, H. Heiberg, T. Helgaker, A. C. Hennum, H. Hettema, E. Hjertenæs, S. Høst, I.-M. Høyvik, M. F. Iozzi, B. Jansík, H. J. A. Jensen, D. Jonsson, P. Jørgensen, J. Kauczor, S. Kirpekar, T. Kjærgaard, W. Klopper, S. Knecht, R. Kobayashi, H. Koch, J. Kongsted, A. Krapp, K. Kristensen, A. Ligabue, O. B. Lutnæs, J. I. Melo, K. V. Mikkelsen, R. H. Myhre, C. Neiss, C. B. Nielsen, P. Norman, J. Olsen, J. M. H. Olsen, A. Osted, M. J. Packer, F. Pawlowski, T. B. Pedersen, P. F. Provasi, S. Reine, Z. Rinkevicius, T. A. Ruden, K. Ruud, V. V. Rybkin, P. Sałek, C. C. M. Samson, A. S. de Merás, T. Saue, S. P. A. Sauer, B. Schimmelpfennig, K. Sneskov, A. H. Steindal, K. O. Sylvester-Hvid, P. R. Taylor, A. M. Teale, E. I. Tellgren, D. P. Tew, A. J. Thorvaldsen, L. Thøgersen, O. Vahtras, M. A. Watson, D. J. D. Wilson, M. Ziolkowski, and H. Ågren, Wiley Interdiscip. Rev.: Comput. Mol. Sci. **4**, 269 (2014).
[9] P. S. Bagus, Phys. Rev. **139**, A619 (1965).
[10] L. Triguero, O. Plashkevych, L. Pettersson, and H. Ågren, J. Electron Spectrosc. Relat. Phenom. **104**, 195 (1999).
[11] O. Plashkevych, H. Ågren, L. Karlsson, and L. Pettersson, J. Electron. Spectrosc. Relat. Phenom. **106**, 51 (2000).
[12] J. P. Perdew and A. Zunger, Phys. Rev. B **23**, 5048 (1981).
[13] G. Tu, Z. Rinkevicius, O. Vahtras, H. Ågren, U. Ekström, P. Norman, and V. Carravetta, Phys. Rev. A **76**, 022506 (2007).
[14] A. Naves de Brito, N. Correia, S. Svensson, and H. Ågren, J. Chem. Phys. **95**, 2965 (1991).
[15] A. Naves de Brito, M. P. Keane, N. Correia, S. Svensson, U. Gelius, and B. J. Lindberg, Surf. Interface Anal. **17**, 94 (1991).
[16] Y. Tu, Q. Zhang, and H. Ågren, J. Phys. Chem. B **111**, 3591 (2007).
[17] G. Beamson, D. T. Clark, and D. S.-L. Law, Surf. Interface Anal. **27**, 76 (1999).
[18] S. Piperno, L. Lozzi, R. Rastelli, M. Passacantando, and S. Santucci, Appl. Surf. Sci. **252**, 5583 (2006).
[19] S. R. Leadley and J. F. Watts, J. Adhes. **60**, 175 (1997).
[20] K. Artyushkova and J. E. Fulghum, Surf. Interface Anal. **31**, 352 (2001).
[21] J. F. Watts, S. R. Leadley, J. E. Castle, and C. J. Blomfield, Langmuir **16**, 2292 (2000).
[22] M. N. Hedhili, B. V. Yakshinskiy, R. Wasielewski, A. Ciszewski, and T. E. Madey, J. Chem. Phys. **128**, 174704 (2008).
[23] L. Gagliardi, R. Lindh, and G. Karlström, J. Chem. Phys. **121**, 4494 (2004).
[24] O. Vahtras, "LoProp for Dalton," (2014), http://dx.doi.org/10.5281/zenodo.13276.
[25] V. Barone and A. Polimeno, Chem. Soc. Rev. **36**, 1724 (2007).

[26] Avogadro: an open-source molecular builder and visualization tool. Version 1.1.1. http://avogadro.openmolecules.net/.
[27] M. D. Hanwell, D. E. Curtis, D. C. Lonie, T. Vandermeersch, E. Zurek, and G. R. Hutchison, J. Cheminf. **4**, 1 (2012).
[28] A. D. Becke, J. Chem. Phys. **98**, 5648 (1993).
[29] W. J. Hehre, R. Ditchfield, and J. A. Pople, J. Chem. Phys. **56**, 2257 (1972).
[30] T. Clark, J. Chandrasekhar, G. W. Spitznagel, and P. V. R. Schleyer, J. Comput. Chem. **4**, 294 (1983).
[31] P. Hariharan and J. Pople, Theor. Chim. Acta **28**, 213 (1973).
[32] M. J. Frisch, G. W. Trucks, H. B. Schlegel, G. E. Scuseria, M. A. Robb, J. R. Cheeseman, G. Scalmani, V. Barone, B. Mennucci, G. A. Petersson, H. Nakatsuji, M. Caricato, X. Li, H. P. Hratchian, A. F. Izmaylov, J. Bloino, G. Zheng, J. L. Sonnenberg, M. Hada, M. Ehara, K. Toyota, R. Fukuda, J. Hasegawa, M. Ishida, T. Nakajima, Y. Honda, O. Kitao, H. Nakai, T. Vreven, J. J. A. Montgomery, J. E. Peralta, F. Ogliaro, M. Bearpark, J. J. Heyd, E. Brothers, K. N. Kudin, V. N. Staroverov, T. Keith, R. Kobayashi, J. Normand, K. Raghavachari, A. Rendell, J. C. Burant, S. S. Iyengar, J. Tomasi, M. Cossi, N. Rega, J. M. Millam, M. Klene, J. E. Knox, J. B. Cross, V. Bakken, C. Adamo, J. Jaramillo, R. Gomperts, R. E. Stratmann, O. Yazyev, A. J. Austin, R. Cammi, C. Pomelli, J. W. Ochterski, R. L. Martin, K. Morokuma, V. G. Zakrzewski, G. A. Voth, P. Salvador, J. J. Dannenberg, S. Dapprich, A. D. Daniels, O. Farkas, J. B. Foresman, J. V. Ortiz, J. Cioslowski, and D. J. Fox, "Gaussian 09, Revision D.01," Gaussian, Inc., Wallingford, CT, 2013.
[33] D. W. Zhang and J. Z. H. Zhang, J. Chem. Phys **119**, 3599 (2003).
[34] P. Sałek, O. Vahtras, T. Helgaker, and H. Ågren, J. Chem. Phys. **117**, 9630 (2002).
[35] P. O. Wildmark, P. Malmqvist, and B. O. Roos, Theor. Chim. Acta. **77**, 291 (1990).
[36] J. M. Olsen, K. Aidas, and J. Kongsted, J. Chem. Theory Comput. **6**, 3721 (2010).
[37] B. Thole, Chem. Phys. **59**, 341 (1981).
[38] P. T. van Duijnen and M. Swart, J. Phys. Chem. A **102**, 2399 (1998).
[39] H. J. A. Jensen, P. Jørgensen, and H. Ågren, J. Chem. Phys. **87**, 451 (1987).
[40] J. Thom H. Dunning, J. Chem. Phys. **90**, 1007 (1989).
[41] D. E. Woon and J. Thom H. Dunning, J. Chem. Phys. **103**, 4572 (1995).
[42] R. A. Kendall, J. Thom H. Dunning, and R. J. Harrison, J. Chem. Phys. **96**, 6796 (1992).
[43] O. Takahashi and L. G. M. Pettersson, J. Chem. Phys. **121**, 10339 (2004).
[44] H. Ågren and G. Karlström, J. Chem. Phys. **79**, 587 (1983).
[45] M. Giesbers, A. T. M. Marcelis, and H. Zuilhof, Langmuir **29**, 4782 (2013).
[46] T. R. Leftwich and A. V. Teplyakov, J. Electron. Spectrosc. Relat. Phenom. **175**, 31 (2009).